HIP-2007-01/TH
KEK-TH-1128
hep-ph/0701155

arXiv:hep-ph/0701155v3 15 Mar 2007

Top quark spin correlations in the Randall-Sundrum model at the CERN Large Hadron Collider

Masato Arai [a] *, **Nobuchika Okada** [b] †, **Karel Smolek** [c] ‡
and
Vladislav Šimák [d] §

[a] *High Energy Physics Division, Department of Physical Sciences, University of Helsinki and Helsinki Institute of Physics, P.O.Box 64, FIN-00014, Finland*

[b] *Theory Division, KEK, Tsukuba, Ibaraki 305-0801, Japan*

[c] *Institute of Experimental and Applied Physics, Czech Technical University in Prague, Horská 3a/22, 128 00 Prague 2, Czech Republic*

[d] *Faculty of Nuclear Sciences and Physical Engineering, Czech Technical University in Prague, Břehová 7, 115 19 Prague 1, Czech Republic*

Abstract

In the Randall-Sundrum model, we study top-antitop pair production and top spin correlations at the Large Hadron Collider. In addition to the Standard Model processes, there is a new contribution to the top-antitop pair production process mediated by graviton Kaluza-Klein modes in the s-channel. We calculate the density matrix for the top-antitop pair production including the new contribution. With a reasonable parameter choice in the Randall-Sundrum model, we find a sizable deviation of the top-antitop pair production cross section and the top spin correlations from those in the Standard Model. In particular, resonant productions of the graviton Kaluza-Klein modes give rise to a remarkable enhancement of such a deviation.

* *masato.arai@helsinki.fi*
† *okadan@post.kek.jp*
‡ *karel.smolek@utef.cvut.cz*
§ *simak@fzu.cz*

1 Introduction

During the past several decades the gauge hierarchy problem has been a guiding principle to propose beyond the standard model (SM), and many new physics models have been proposed to solve this problem. Brane world scenario recently proposed provides a possible solution for this problem. In this scenario whole space has more than three spatial dimensions and the SM fields are confined on a 4-dimensional hypersurface called "D3-brane". There are two typical models based on this setup. One is the so-called ADD model proposed by Arkani-Hamed, Dimopoulos and Dvali (ADD) [1]. In this model, there are n-extra dimensions compactified on n-torus with common radius R and a D3-brane embedded in $(4+n)$-dimensional bulk is introduced on which the SM fields reside. This setup gives a relation $M_{\rm pl} = M_{\rm D}(M_{\rm D}R)^{n/2}$ between the 4-dimensional Planck mass $M_{\rm pl}$ and the Planck scale of $(4+n)$-dimensions $M_{\rm D}$. If the compactification radius is large enough (for instance, $R \sim 0.1$ mm for $n = 2$), M_D can be $\mathcal{O}(1$ TeV) and thus one obtains a solution to the gauge hierarchy problem. In fact, this picture is consistent with the current experimental bound on R around 200 μm [2].

The other model was proposed by Randall and Sundrum (RS) [3]. This is a 5-dimensional model, where one extra-dimension is compactified on a $\mathbf{S}^1/Z_2$ orbifold and a negative cosmological constant is introduced in the bulk. Two D3-branes are placed at fixed points of the orbifold $\phi = 0$ and $\phi = \pi$ (ϕ is an angle of $\mathbf{S}^1$) with opposite brane tensions. A brane at $\phi = 0$ with a positive tension is called the hidden brane and the other one at $\phi = \pi$ with a negative tension is called the visible brane on which the SM fields are confined. Solving the Einstein equation of this system, the 5-dimensional bulk geometry is found to be a slice of anti-de Sitter (AdS_5) space,

$$ds^2 = e^{-2\kappa r_c|\phi|}\eta_{\mu\nu}dx^\mu dx^\nu - r_c^2 d\phi^2\,, \quad \eta_{\mu\nu} = \mathrm{diag}(1,-1,-1,-1)\,, \tag{1.1}$$

where κ is the AdS curvature in five dimensions, and r_c is a compactification radius. This background geometry allows us to take the Planck scale as a fundamental scale. Indeed, in effective 4-dimensional description an effective mass scale on the visible brane is warped down such as $\Lambda_\pi = \bar{M}_{\rm pl}e^{-\pi\kappa r_c}$ due to effect of the warped geometry, where $\bar{M}_{\rm pl}$ is the reduced Planck mass. Therefore, with a mild parameter tuning, $\kappa r_c \simeq 12$, we can realize $\Lambda_\pi = \mathcal{O}(1$ TeV) and obtain a natural solution to the gauge hierarchy problem.

In the brane world scenario, an infinite tower of Kaluza-Klein (KK) gravitons appears in

effective 4-dimensional theory. Effective couplings between these KK gravitons and the SM fields are controlled by M_D or Λ_π in each typical model. Since these mass scales should be around TeV so as to solve the gauge hierarchy problem, we can expect new phenomena induced by the KK gravitons, for example, direct KK graviton emission process and virtual KK graviton exchange process at high energy collisions. In particular, the virtual KK graviton exchange process is interesting, because it can give rise to characteristic angular distributions and spin configurations for outgoing particles, which reflect the spin-2 nature of the intermediate KK gravitons.

One of good candidates to study a spin configuration is a top-antitop quark pair, since the top quark, with mass in the range of 175 GeV [5], decays electroweakly before hadronizing [6]. A possible spin polarization of the top-antitop quark pair is directly transferred to its decay products and therefore there are significant angular correlations between the top quark spin axis and the direction of motion of the decay products. The spin correlations for the hadronic top-antitop pair production process have been extensively studied in the quantum chromodynamics (QCD) [8, 9, 10]. It is found that there is a spin asymmetry between the produced top-antitop pairs, namely, the number of produced top-antitop quark pairs with both spin up or spin down (like pair) is different from the number of pairs with the opposite spin combinations (unlike pair). If the top quark is coupled to a new physics beyond the SM, the top-antitop spin correlations could be altered. Therefore, the top-antitop spin correlations can provide useful information to test not only the SM but also a possible new physics at hadron colliders. The Large Hadron Collider (LHC) has a big advantage to study the top spin correlations, since it will produce almost 10 millions of top quarks a year (during its low luminosity run).

In Ref. [11], effect of the KK gravitons on the top spin correlations in the ADD model at the LHC was studied. A sizable deviation of the top spin correlations from the SM one was found with scale M_D below 2 TeV. The purpose of this paper is to study the top spin correlations in the RS model at the LHC. To study this issue in the RS model is more motivated than in the ADD model by the following reasons. In the ADD model, a mass difference of each KK graviton is characterized by the radius of the extra dimensions (R^{-1} $\sim$meV for $n = 2$), which is much smaller than detector resolutions and it is impossible to identify each resonant KK graviton at collider experiments. In fact, couplings between each KK graviton and the SM fields are suppressed

by the 4-dimensional Planck mass and extremely weak. After coherently summing up many KK graviton processes, the KK graviton effects can be sizable. However, there is a theoretical problem in the ADD model with two or more extra dimensions: Sum of all intermediate KK gravitons diverges and is not well-defined. Although this problem can be solved by introducing a finite brane tension [12] or a finite brane width [13], which give rise to a physical ultraviolet cutoff and make the sum finite, a new parameter (the brane tension or the width of the brane) is brought into a model. On the other hand, in the RS model only one extra dimension is introduced, and sum of all intermediate KK gravitons turns out to be finite and the KK graviton mediated process is well-defined at low energies. Each KK graviton strongly couples to the SM fields with Λ_π suppressed couplings, and KK graviton mass is characterized by $\kappa e^{-\kappa r_c \pi} \sim$ TeV. As a result, we can expect a resonant production of the KK gravitons at colliders if the collider energy is high enough. This is a direct signal of the RS model. Furthermore, the resonance gives rise to an enhancement of production of the top-antitop pairs and provides a big statistical advantage for studying the top spin correlations around the resonance pole.

This paper is organized as follows. In section 2, we briefly review the top spin correlations. In section 3, we examine the invariant amplitudes for the polarized top-antitop pair production processes, $q\bar{q} \to t\bar{t}$, $gg \to t\bar{t}$ mediated by virtual KK gravitons in the s-channel. We perform numerical analysis in section 4. Section 5 is devoted to conclusions. In Appendices, the coefficient of the KK graviton decay width and the density matrix are shown.

2 Spin correlation

At hadron collider, the top-antitop quark pair is produced through the processes of quark-antiquark pair annihilation and gluon fusion:

$$i \to t + \bar{t}, \;\; i = q\bar{q}\,, gg\,. \tag{2.1}$$

The former is the dominant process at the Tevatron, while the latter is dominant at the LHC. The produced top-antitop pairs decay before hadronization takes place. The main decay modes in the SM involve leptonic and hadronic modes:

$$t \to bW^+ \to bl^+\nu_l\,, bu\bar{d}\,, bc\bar{s}, \tag{2.2}$$

where $l = e, \mu, \tau$. The differential decay rates to a decay product $f = b, l^+, \nu_l$, etc. at the top quark rest frame can be parameterized as

$$\frac{1}{\Gamma}\frac{d\Gamma}{d\cos\theta_f} = \frac{1}{2}(1 + \kappa_f \cos\theta_f), \tag{2.3}$$

where Γ is the partial decay width of the respective decay channel and θ_f is the angle between the top quark polarization and the direction of motion of the decay product f at the top quark rest frame. The coefficient κ_f called top spin analyzing power is a constant between -1 and 1. The ability to distinguish the polarization of the top quark evidently increases with κ_f. The most powerful spin analyzer is a charged lepton, for which $\kappa_{l^+} = +1$ at tree level [14]. Other values of κ_f are $\kappa_b = -0.41$ for the b-quark and $\kappa_{\nu_l} = -0.31$ for the ν_l, respectively. In hadronic decay modes, the role of the charged lepton is replaced by the d or s quark.

Now we see how the top spin correlations appear in the chain of processes of $i \to t\bar{t}$ and decay of the top quarks. The total matrix element squared for the top-antitop pair production (2.1) and their decay channels (2.2) is given by

$$|\mathcal{M}|^2 \propto \mathrm{Tr}[\rho R^i \bar{\rho}] = \rho_{\alpha'\alpha} R^i_{\alpha\beta,\alpha'\beta'} \bar{\rho}_{\beta'\beta} \tag{2.4}$$

in the narrow-width approximation for the top quark. Here the subscripts denote the top and antitop spin indices, and R^i denotes the density matrix corresponding to the production of the on-shell top-antitop quark pair through the process i in (2.1):

$$R^i_{\alpha\beta,\alpha'\beta'} = \sum_{\text{initial spin}} \mathcal{M}(i \to t_\alpha \bar{t}_\beta)\mathcal{M}^*(i \to t_{\alpha'} \bar{t}_{\beta'}), \tag{2.5}$$

where $\mathcal{M}(i \to t_\alpha \bar{t}_\beta)$ is the amplitude for the top-antitop pair production. The matrices ρ and $\bar{\rho}$ are the density matrices corresponding to the decays of polarized top and antitop quarks into some final states at the top and antitop rest frame, respectively. In the leptonic decay modes, the matrices ρ, which lead to (2.3), can be obtained as (see, for instance, [7])

$$\rho_{\alpha'\alpha} = \mathcal{M}(t_\alpha \to b l^+ \nu_l)\mathcal{M}^*(t_{\alpha'} \to b l^+ \nu_l) = \frac{\Gamma}{2}(1 + \kappa_f \vec{\sigma} \cdot \vec{q}_f)_{\alpha'\alpha}, \tag{2.6}$$

where q_f is the unit vector of the direction of motion of the decay product f. The density matrix for the polarized antitop quark is obtained by replacing $\kappa_f \to -\kappa_f$ in (2.6) if there is no CP violation. In the SM, there is no CP violation in the top quark decay at the leading order. In the RS model we consider, there is no CP violation at the leading order, and this relation holds.

The best way to analyze the top-antitop spin correlations is to see the angular correlations of two charged leptons l^+l^- produced by the top-antitop quark leptonic decays. In the following, we consider only the leptonic decay channels. Using (2.4)-(2.6) and integrating over the azimuthal angles of the charged leptons, we obtain the following double distribution [8, 9, 10]

$$\frac{1}{\sigma}\frac{d^2\sigma}{d\cos\theta_{l^+}d\cos\theta_{l^-}} = \frac{1}{4}\left(1 + B_1\cos\theta_{l^+} + B_2\cos\theta_{l^-} - C\cos\theta_{l^+}\cos\theta_{l^-}\right). \tag{2.7}$$

Here σ denotes the cross section for the process of the leptonic decay modes, and $\theta_{l^+}(\theta_{l^-})$ denotes the angle between the top (antitop) spin axis and the direction of motion of the antilepton (lepton) at the top (antitop) rest frame. In the following analysis, we use the helicity spin basis which is almost optimal one to analyze the top spin correlation at the LHC.[1] In this basis, the top (antitop) spin axis is regarded as the direction of motion of the top (antitop) in the top-antitop center-of-mass system. The coefficients B_1 and B_2 are associated with a possible polarization of the (anti)top quark transverse to the production plane in proton-proton (or proton-antiproton) collision, called a transverse polarization, and C encodes the top spin correlations, whose explicit expression is given by

$$C = \mathcal{A}\kappa_{l^+}\kappa_{l^-}, \quad \kappa_{l^+} = \kappa_{l^-} = 1\,, \tag{2.8}$$

where the coefficient $\mathcal{A}$ represents the spin asymmetry between the produced top-antitop pairs with like and unlike spin pairs defined as

$$\mathcal{A} = \frac{\sigma(t_\uparrow\bar{t}_\uparrow) + \sigma(t_\downarrow\bar{t}_\downarrow) - \sigma(t_\uparrow\bar{t}_\downarrow) - \sigma(t_\downarrow\bar{t}_\uparrow)}{\sigma(t_\uparrow\bar{t}_\uparrow) + \sigma(t_\downarrow\bar{t}_\downarrow) + \sigma(t_\uparrow\bar{t}_\downarrow) + \sigma(t_\downarrow\bar{t}_\uparrow)}. \tag{2.9}$$

Here $\sigma(t_\alpha\bar{t}_\beta)$ is the cross section of the top-antitop pair production at parton level with denoted spin indices.

In the SM, there is no transverse polarization, $B_1 = B_2 = 0$ at the leading order of ${\alpha_s}^2$ while the spin asymmetry is found to be $\mathcal{A} = +0.319$ for the LHC. [3] At the LHC in the ATLAS

[1] Recently another spin basis was constructed, which has a larger spin correlation than the helicity basis at the LHC [15].

[2] At the one-loop level, the transverse polarization is induced. Detailed analysis has been performed in Refs. [16] and [17].

[3] The parton distribution function set of CTEQ6L [18] has been used in our calculations. The resultant spin asymmetry somewhat depends on the parton distribution functions used.

experiment, the spin asymmetry of the top-antitop pairs will be measured with a precision of several percent, even after one LHC year at low luminosity (10 fb^{-1}) [19]. Since in the brane world scenario there is a new contribution to the top-antitop production process through virtual KK graviton exchange in the s-channel, the spin asymmetry could be altered from the SM one. It is found that in the ADD model, the KK graviton contribution reduces the spin asymmetry [11], for example, $\mathcal{A} = +0.147$ for $M_D = 1$ TeV. In the next section, we calculate the squared amplitude for the top-antitop pair production including the virtual KK graviton mediated process in the RS model and evaluate the spin asymmetry at tree level, assuming that loop corrections in the RS model will not give a significant contribution.

3 Scattering amplitude in the RS model

In the RS model, because of the warped metric, zero-mode graviton and KK gravitons have different non-trivial configurations with respect to the fifth dimensional coordinates. In particular, the KK gravitons are localizing around the visible brane and so couplings between the KK gravitons and the SM fields are enhanced. The effective interaction Lagrangian is given by [4]

$$\mathcal{L}_{\rm int} = -\frac{1}{\bar{M}_{\rm pl}} T^{\mu\nu}(x) h^{(0)}_{\mu\nu}(x) - \frac{1}{\Lambda_\pi} T^{\mu\nu}(x) \sum_{n=1}^{\infty} h^{(n)}_{\mu\nu}(x)\,, \tag{3.1}$$

where $h^{(n)}_{\mu\nu}$ is the n-th graviton KK mode, $T^{\mu\nu}$ is the energy-momentum tensor of the SM fields on the visible brane, and $\Lambda_\pi = \bar{M}_{\rm pl} e^{-\kappa r_c \pi} \sim$ TeV. The graviton zero mode couples with the usual strength and its effect is of course negligible for collider physics, while each graviton KK mode strongly couples to the SM fields with the suppression factor Λ_π^{-1}.

Mass spectrum of the KK gravitons is determined by the relation

$$m_n = x_n \kappa e^{-\kappa r_c \pi}\,, \tag{3.2}$$

where x_n is a root of the Bessel function of the first order, $J_1(x_n) = 0$, and $x_1 \sim 3.83$, $x_2 \sim 7.02$, $x_3 \sim 10.17$, for example. Assuming that the 5-dimensional curvature κ is small compared to M where M is the 5-dimensional Planck scale, the lightest KK graviton mass appears around several hundred GeV which is accessible by the LHC. Once the lightest KK graviton mass is fixed, higher KK graviton mass can be determined by using given numerical factors, $m_n = m_1(x_n/x_1)$. Using

m_1, the effective scale Λ_π can be rewritten as

$$\Lambda_\pi = \frac{m_1}{3.83}\left(\frac{\bar{M}_{\rm pl}}{\kappa}\right). \tag{3.3}$$

In our numerical analysis, we use m_1 and $\kappa/\bar{M}_{\rm pl}$ as input parameters. As mentioned above, we assume the 5-dimensional curvature κ is much smaller than M, whose condition is actually necessary to trust the RS metric. It yields the bound for the input parameter as $\kappa/\bar{M}_{\rm pl} < 0.1$ [4].

The effective interaction Eq. (3.1) leads to the top-antitop pair production through the virtual KK graviton exchange in the s-channel. The invariant amplitude in momentum space is obtained as[4]

$$\mathcal{M}_G = A(s)T^{\mu\nu}(k_1,k_2)T_{\mu\nu}(k_3,k_4)\,, \tag{3.4}$$

$$A(s) \equiv -\frac{1}{\Lambda_\pi^2}\sum_{n=1}^{\infty}\frac{1}{s^2-m_n^2+im_n\Gamma_n}\,, \tag{3.5}$$

with $s=(k_1+k_2)^2=(k_3+k_4)^2$. Here Γ_n is the total decay width of the n-th KK graviton given by

$$\Gamma_n(h^{(n)}\to yy) = \frac{m_n x_n^2}{16\pi}\left(\frac{\kappa}{\bar{M}_{\rm pl}}\right)^2\sum_y \Delta_n^{yy}\,, \tag{3.6}$$

where Δ_n^{yy} is a dimensionless coefficient for each decay mode, and its exact form is listed in Appendix A.

In the center-of-mass frame, we can straightforwardly calculate the density matrix $R^i_{\alpha\beta,\alpha'\beta'}$ including both the SM (QCD) and the virtual KK-graviton contributions. It is sufficient to calculate its diagonal part since only the diagonal part is relevant to the spin asymmetry (2.9) (full density matrix is shown in Appendix B). For the $q\bar{q}$ initial state we find

$$\begin{aligned}|\mathcal{M}(q\bar{q}\to t_\uparrow\bar{t}_\uparrow)|^2 &= |\mathcal{M}(q\bar{q}\to t_\downarrow\bar{t}_\downarrow)|^2 \\ &= \frac{g^4}{9}(1-\beta^2)\sin^2\theta + \frac{|A(s)|^2s^4\beta^2}{128}(1-\beta^2)\sin^2 2\theta\,, \end{aligned}\tag{3.7}$$

$$\begin{aligned}|\mathcal{M}(q\bar{q}\to t_\uparrow\bar{t}_\downarrow)|^2 &= |\mathcal{M}(q\bar{q}\to t_\downarrow\bar{t}_\uparrow)|^2 \\ &= \frac{g^4}{9}(1+\cos^2\theta) + \frac{|A(s)|^2s^4\beta^2}{128}(\cos^2 2\theta+\cos^2\theta)\,, \end{aligned}\tag{3.8}$$

[4] This is easily reproduced by the replacement in a corresponding formula in the ADD model: $\frac{4\pi\lambda}{M_D^4} \to -\frac{1}{\Lambda_\pi^2}\sum_{n=1}^{\infty}\frac{1}{s-m_n^2}$ in the normalization of Ref. [11].

where θ is the scattering angle between the incoming q and outgoing t, g is a strong coupling constant, and $\beta = \sqrt{1-4m_t^2/s}$ with top quark mass m_t. For the gg initial state we obtain

$$\begin{aligned}|\mathcal{M}(gg \to t_\uparrow \bar{t}_\uparrow)|^2 &= |\mathcal{M}(gg \to t_\downarrow \bar{t}_\downarrow)|^2 \\ &= \frac{g^4\beta^2}{96}\mathcal{Y}(\beta,\cos\theta)(1-\beta^2)(1+\beta^2+\beta^2\sin^4\theta) + \mathcal{Z}(\beta,\theta,s)s^2\beta^2(1-\beta^2)\sin^4\theta\,,\end{aligned} \tag{3.9}$$

$$\begin{aligned}|\mathcal{M}(gg \to t_\uparrow \bar{t}_\downarrow)|^2 &= |\mathcal{M}(q\bar{q} \to t_\downarrow \bar{t}_\uparrow)|^2 \\ &= \frac{g^4\beta^2}{96}\mathcal{Y}(\beta,\cos\theta)\sin^2\theta(1+\cos^2\theta) + \mathcal{Z}(\beta,\theta,s)s^2\beta^2\sin^2\theta(1+\cos^2\theta)\,.\end{aligned} \tag{3.10}$$

Here $\mathcal{Y}(\beta,\theta,s)$ and $\mathcal{Z}(\beta,\theta,s)$ are defined by

$$\mathcal{Y}(\beta,\cos\theta) = \frac{7+9\beta^2\cos^2\theta}{(1-\beta^2\cos^2\theta)^2}\,, \tag{3.11}$$

$$\mathcal{Z}(\beta,\theta,s) = \frac{1}{32}\left(-\frac{g^2}{1-\beta^2\cos^2\theta}\mathrm{Re}(A(s)) + \frac{3}{8}|A(s)|^2 s^2\right)\,, \tag{3.12}$$

respectively. As in the same with the ADD case discussed in Ref. [11], there is no interference term for the quark-antiquark pair annihilation process, while there is the non-vanishing interference in the gluon fusion process.

With the squared amplitudes Eqs. (3.7)-(3.10), one can find the integrated top-antitop quark pair production cross section through the formula,

$$\begin{aligned}\sigma_{tot}(pp \to t_\alpha \bar{t}_\beta) = \sum_{a,b}\int dx_1 \int dx_2 \int d\cos\theta f_a(x_1,Q^2) f_b(x_2,Q^2) \\ \times \frac{d\sigma(a(x_1 E_{\rm CMS}/2)b(x_2 E_{\rm CMS}/2) \to t_\alpha \bar{t}_\beta)}{d\cos\theta}\,,\end{aligned} \tag{3.13}$$

where f_a denotes the parton distribution function for a parton a, $E_{\rm CMS}$ is a center-of-mass energy of a proton-proton system, and Q is a factorization scale.

Using above formulas, we calculate the double distribution (2.7) in the RS model. Explicit calculation tells us that the transverse polarization is vanishing, i.e. $B_1 = B_2 = 0$ in the RS model while the spin asymmetry $\mathcal{A}$ is altered from the SM one.

4 Numerical results

Here we show various numerical results and demonstrate interesting properties of measurable quantities in the RS model. In our analysis we use the parton distribution functions of CTEQ6L [18] with the factorization scale $Q = m_t = 175$ GeV, $N_f = 5$ and $\alpha_s(Q) = 0.1074$. As mentioned above, we choose m_1 and $\kappa/\bar{M}_{\rm pl}$ as input parameters. In practice, we fix $m_1 = 600$ GeV, subsequently $m_2 = 1099$, $m_3 = 1582$, $m_4 = 2686$ GeV etc.

In Figs. 1 and 2, the cross sections of the top-antitop pair production through $q\bar{q} \to t\bar{t}$ (Fig. 1) and $gg \to t\bar{t}$ (Fig. 2) at the parton level are depicted as a function of parton center-of-mass energy $\sqrt{s} = M_{t\bar{t}}$ for $m_1 = 600$ GeV and various $\kappa/\bar{M}_{\rm pl}$. The SM cross section decreases, while the cross section of the RS model grows rapidly with $\sqrt{s}$ and thus the unitarity will be violated at high energies. This behavior can be understood from the formulas of the squared amplitudes Eqs. (3.7)-(3.10). Peaks in the figures correspond to resonant productions of KK gravitons. Total cross sections and the width of each peak become larger, as $\kappa/\bar{M}_{\rm pl}$ is taken to be large.

Differential cross section for the top-antitop pair production given by

$$\frac{d\sigma_{tot}(pp \to t\bar{t})}{d\cos\theta} = \sum_{a,b} \int dx_1 \int dx_2 \, f_a(x_1, Q^2) f_b(x_2, Q^2) \frac{d\sigma(t\bar{t})}{d\cos\theta} \tag{4.1}$$

is shown in Fig. 3 with $E_{CMS} = 14$ TeV. Here, the decomposition of the total cross section into the like $(t_\uparrow \bar{t}_\uparrow + t_\downarrow \bar{t}_\downarrow)$ and the unlike $(t_\uparrow \bar{t}_\downarrow + t_\downarrow \bar{t}_\uparrow)$ top-antitop spin pairs in the RS model are also shown.

We are also interested in the dependence of the cross section on the top-antitop invariant mass $M_{t\bar{t}} = \sqrt{(p_t + p_{\bar{t}})^2}$ where $p_t(p_{\bar{t}})$ is momentum of (anti)top quark. This is given by

$$\frac{d\sigma_{tot}(pp \to t\bar{t})}{dM_{t\bar{t}}} = \sum_{a,b} \int_{-1}^{1} d\cos\theta \int_{\frac{M_{t\bar{t}}^2}{E_{CMS}^2}}^{1} dx_1 \frac{2M_{t\bar{t}}}{x_1 E_{CMS}^2} f_a(x_1, Q^2) f_b\left(\frac{M_{t\bar{t}}^2}{x_1 E_{CMS}^2}, Q^2\right) \frac{d\sigma(t\bar{t})}{d\cos\theta}. \tag{4.2}$$

The result for $m_1 = 600$ GeV and $\kappa/\bar{M}_{\rm pl} = 0.1$ is shown in Fig. 4. The deviation of the cross section in the RS model from the one in the SM grows as s becomes large. Cross sections for the like and the unlike top-antitop spin pairs in the RS model are also shown. The differential cross section as a function of the center-of-mass energy of colliding partons for various $\kappa/\bar{M}_{\rm pl}$ is depicted in Fig. 5. Deviation from the SM one becomes large according to $\kappa/\bar{M}_{\rm pl}$.

Now let us show the result for the spin asymmetry $\mathcal{A}$. In Fig. 6, the spin asymmetry as a function of the center-of-mass energy of colliding partons for various $\kappa/\bar{M}_{\rm pl}$ is depicted. Deviation from the SM one becomes larger as the center-of-mass energy and $\kappa/\bar{M}_{\rm pl}$ become larger. As expected, deviation is enhanced around the poles of KK graviton resonances. This implies that we can expect a big statistical advantage for the study of the top spin correlations when we analyze experimental data around a pole. This fact is a crucial difference from the ADD model, where no resonance of KK gravitons can be seen. In Fig. 7 we show the spin asymmetry $\mathcal{A}$ at the LHC, as a function of $\kappa/\bar{M}_{\rm pl}$. We can see a sizable deviation from the SM one, for example, $\mathcal{A} = 0.260$ for $\kappa/\bar{M}_{\rm pl} = 0.1$.

5 Conclusions

In the RS model, we have studied the top-antitop pair production and the top spin correlations at the LHC. In addition to the Standard Model processes, there is a new contribution to the top-antitop pair production process mediated by graviton Kaluza-Klein modes in the s-channel. We have computed the corresponding density matrix for the top-antitop pair production including the new contribution. We have shown various numerical results for the production cross sections and the top spin correlations with input parameters m_1 and $\kappa/\bar{M}_{\rm pl}$ in the RS model. We have found a sizable deviation of the top-antitop pair production cross section and the top spin correlations from those in the Standard Model. In particular, resonant productions of the Kaluza-Klein gravitons give rise to a remarkable enhancement of such deviations. This is a crucial difference from the case in the ADD model.

Acknowledgements

The work of M.A. is supported by the bilateral program of Japan Society for the Promotion of Science and Academy of Finland, "Scientist Exchanges". The work of N.O. is supported in part by Scientific Grants from the Ministry of Education and Science of Japan.

A The coefficients Δ_n^{yy}

Explicit forms of the coefficients Δ_n^{yy} are listed below.

$$\Delta_n^{\gamma\gamma} = \frac{1}{5}, \tag{A.1}$$

$$\Delta_n^{gg} = \frac{8}{5}, \tag{A.2}$$

$$\Delta_n^{WW} = \frac{2}{5}\sqrt{1-4r_W}\left(\frac{13}{12}+\frac{14}{3}r_W+4r_W^2\right), \tag{A.3}$$

$$\Delta_n^{ZZ} = \frac{1}{5}\sqrt{1-4r_Z}\left(\frac{13}{12}+\frac{14}{3}r_Z+4r_Z^2\right), \tag{A.4}$$

$$\Delta_n^{HH} = \frac{1}{30}(1-4r_H)^{5/2}, \tag{A.5}$$

$$\Delta_n^{\nu\bar{\nu}} = \frac{1}{10}, \tag{A.6}$$

$$\Delta_n^{l\bar{l}} = \frac{1}{10}(1-4r_l)^{3/2}\left(1+\frac{8}{3}r_l\right), \tag{A.7}$$

$$\Delta_n^{q\bar{q}} = \frac{3}{10}(1-4r_q)^{3/2}\left(1+\frac{8}{3}r_l\right), \tag{A.8}$$

where $r_y = m_y^2/m_n^2$ for each SM particle y. Expressions for leptons and quarks are for one flavor.

B Density matrix $R^i_{\alpha\beta,\alpha'\beta'}$

In this appendix, we give the full representation of the density matrix for the top antitop pair production in the RS model. For the $q\bar{q} \to t\bar{t}$ process, we find

$$\begin{aligned} R^q_{\uparrow\uparrow,\uparrow\uparrow} &= R^q_{\downarrow\downarrow,\downarrow\downarrow} = -R^q_{\uparrow\uparrow,\downarrow\downarrow} = -R^q_{\downarrow\downarrow,\uparrow\uparrow} \\ &= \frac{g_s^4}{9}(1-\beta^2)\sin^2\theta + \frac{s^4\beta^2}{128}|A(s)|^2(1-\beta^2)\sin^2 2\theta, \end{aligned} \tag{B.1}$$

$$\begin{aligned} R^q_{\uparrow\uparrow,\uparrow\downarrow} &= R^q_{\uparrow\uparrow,\downarrow\uparrow} = R^q_{\uparrow\downarrow,\uparrow\uparrow} = R^q_{\downarrow\uparrow,\uparrow\uparrow} = -R^q_{\uparrow\downarrow,\downarrow\downarrow} = -R^q_{\downarrow\uparrow,\downarrow\downarrow} = -R^q_{\downarrow\downarrow,\uparrow\downarrow} = -R^q_{\downarrow\downarrow,\downarrow\uparrow} \\ &= \frac{g_s^4}{9}\sqrt{1-\beta^2}\sin\theta\cos\theta - \frac{s^4\beta^2}{32}\mathrm{Re}(A(s))\sqrt{1-\beta^2}\sin 4\theta, \end{aligned} \tag{B.2}$$

$$R^q_{\uparrow\downarrow,\uparrow\downarrow} = R^q_{\downarrow\uparrow,\downarrow\uparrow} = \frac{g_s^4}{9}(1+\cos^2\theta) + \frac{s^4\beta^2}{128}|A(s)|^2(\cos^2 2\theta + \cos^2\theta), \tag{B.3}$$

$$R^q_{\uparrow\downarrow,\downarrow\uparrow} = R^q_{\downarrow\uparrow,\uparrow\downarrow} = \frac{g_s^4}{9}(-1+\cos^2\theta) + \frac{s^4\beta^2}{16}\mathrm{Re}(A(s))(1+2\cos 2\theta)\sin^2\theta, \tag{B.4}$$

and, for the $gg \to t\bar{t}$ process,

$$R^g_{\uparrow\uparrow,\uparrow\uparrow} = R^g_{\downarrow\downarrow,\downarrow\downarrow}$$

$$= \left(\frac{g_s^4}{96}\mathcal{Y}(\beta,\cos\theta)(1+\beta^2+\beta^2\sin^4\theta)+\mathcal{Z}(\beta,\theta,s)s^2\sin^4\theta\right)\beta^2(1-\beta^2), \quad \text{(B.5)}$$

$$R^g_{\uparrow\uparrow,\downarrow\downarrow} = R^g_{\downarrow\downarrow,\uparrow\uparrow}$$
$$= -\left(\frac{g_s^4}{96}\mathcal{Y}(\beta,\cos\theta)(-1+\beta^2+\beta^2\sin^4\theta)+\mathcal{Z}(\beta,\theta,s)s^2\sin^4\theta\right)\beta^2(1-\beta^2), \quad \text{(B.6)}$$

$$R^g_{\uparrow\uparrow,\uparrow\downarrow} = R^g_{\uparrow\uparrow,\downarrow\uparrow} = R^g_{\uparrow\downarrow,\uparrow\uparrow} = R^g_{\downarrow\uparrow,\uparrow\uparrow} = -R^g_{\uparrow\downarrow,\downarrow\downarrow} = -R^g_{\downarrow\uparrow,\downarrow\downarrow} = -R^g_{\downarrow\downarrow,\uparrow\downarrow} = -R^g_{\downarrow\downarrow,\downarrow\uparrow}$$
$$= \left(\frac{g_s^4}{96}\mathcal{Y}(\beta,\cos\theta)\cos\theta+\mathcal{Z}(\beta,\theta,s)s^2\right)\beta^2\sqrt{1-\beta^2}\cos\theta\sin^3\theta, \quad \text{(B.7)}$$

$$R^g_{\uparrow\downarrow,\uparrow\downarrow} = R^g_{\downarrow\uparrow,\downarrow\uparrow} = \left(\frac{g_s^4}{96}\mathcal{Y}(\beta,\cos\theta)+\mathcal{Z}(\beta,\theta,s)s^2\right)\beta^2(1+\cos^2\theta)\sin^2\theta, \quad \text{(B.8)}$$

$$R^g_{\uparrow\downarrow,\downarrow\uparrow} = R^g_{\downarrow\uparrow,\uparrow\downarrow} = -\left(\frac{g_s^4}{96}\mathcal{Y}(\beta,\cos\theta)+\mathcal{Z}(\beta,\theta,s)s^2\right)\beta^2\sin^4\theta, \quad \text{(B.9)}$$

where the functions $\mathcal{Y}(\beta,\cos\theta)$ and $\mathcal{Z}(\beta,\theta,s)$ are defined in (3.11) and (3.12).

References

[1] N. Arkani-Hamed, S. Dimopoulos and G. R. Dvali, Phys. Lett. B **429** (1998) 263 [arXiv:hep-ph/9803315]; I. Antoniadis, N. Arkani-Hamed, S. Dimopoulos and G. R. Dvali, Phys. Lett. B **436** (1998) 257 [arXiv:hep-ph/9804398].

[2] J. C. Long, H. W. Chan, A. B. Churnside, E. A. Gulbis, M. C. M. Varney and J. C. Price, Nature **421**, 922 (2003).

[3] L. Randall and R. Sundrum, Phys. Rev. Lett. **83** (1999) 3370 [arXiv:hep-ph/9905221]; Phys. Rev. Lett. **83** (1999) 4690 [arXiv:hep-th/9906064].

[4] H. Davoudiasl, J. L. Hewett and T. G. Rizzo, Phys. Rev. Lett. **84** (2000) 2080 [arXiv:hep-ph/9909255]; Phys. Rev. D **63** (2001) 075004 [arXiv:hep-ph/0006041].

[5] F. Abe *et al.* [CDF Collaboration], Phys. Rev. Lett. **74**, 2626 (1995) [arXiv:hep-ex/9503002].

[6] I. I. Y. Bigi, Y. L. Dokshitzer, V. A. Khoze, J. H. Kühn and P. M. Zerwas, Phys. Lett. B **181**, 157 (1986).

[7] W. Bernreuther, O. Nachtmann, P. Overmann and T. Schröder, Nucl. Phys. B **388**, 53 (1992) [Erratum-ibid. B **406**, 516 (1993)]; A. Brandenburg and J. P. Ma, Phys. Lett. B **298**, 211 (1993).

[8] T. Stelzer and S. Willenbrock, Phys. Lett. B **374**, 169 (1996) [arXiv:hep-ph/9512292]; A. Brandenburg, Phys. Lett. B **388**, 626 (1996) [arXiv:hep-ph/9603333]; D. Chang, S. C. Lee and A. Sumarokov, Phys. Rev. Lett. **77**, 1218 (1996) [arXiv:hep-ph/9512417].

[9] G. Mahlon and S. J. Parke, Phys. Rev. D **53**, 4886 (1996) [arXiv:hep-ph/9512264]; G. Mahlon and S. J. Parke, Phys. Lett. B **411**, 173 (1997) [arXiv:hep-ph/9706304].

[10] W. Bernreuther, A. Brandenburg, Z. G. Si and P. Uwer, Phys. Rev. Lett. **87**, 242002 (2001) [arXiv:hep-ph/0107086]; W. Bernreuther, A. Brandenburg, Z. G. Si and P. Uwer, Nucl. Phys. B **690**, 81 (2004) [arXiv:hep-ph/0403035].

[11] M. Arai, N. Okada, K. Smolek and V. Šimák, Phys. Rev. D **70** (2004) 115015 [arXiv:hep-ph/0409273].

[12] M. Bando, T. Kugo, T. Noguchi and K. Yoshioka, Phys. Rev. Lett. **83**, 3601 (1999) [arXiv:hep-ph/9906549].

[13] J. Hisano and N. Okada, Phys. Rev. D **61**, 106003 (2000) [arXiv:hep-ph/9909555].

[14] A. Czarnecki, M. Jezabek and J. H. Kühn, Nucl. Phys. B **351** (1991) 70.

[15] P. Uwer, Phys. Lett. B **609** (2005) 271 [arXiv:hep-ph/0412097].

[16] W. G. D. Dharmaratna and G. R. Goldstein, Phys. Rev. D **41** (1990) 1731; preprint TUFIX-TH-92-GO2 (1992), unpublished.

[17] W. Bernreuther, A. Brandenburg and P. Uwer, Phys. Lett. B **368** (1996) 153 [arXiv:hep-ph/9510300].

[18] J. Pumplin *et al.*, JHEP **07** (2002) 012 [arXiv:hep-ph/0201195].

[19] F. Hubaut, E. Monnier, P. Pralavorio, V. Šimák, K. Smolek, Eur. Phys. J. C **44** (2005) 13 [arXiv:hep-ex/0508061].

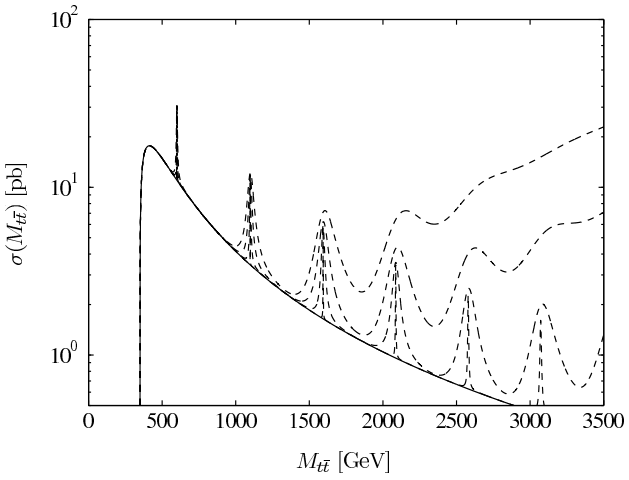

Figure 1: The dependence of the cross section of the top-antitop quark pair production by quark-antiquark pair annihilation on the center-of-mass energy of colliding partons. The solid line and dashed lines correspond to the results of the SM and the RS model for $m_1 = 600$ GeV and $\kappa/\bar{M}_{\rm pl} = 0.01, 0.04, 0.07$ and 0.1 from bottom to top, respectively.

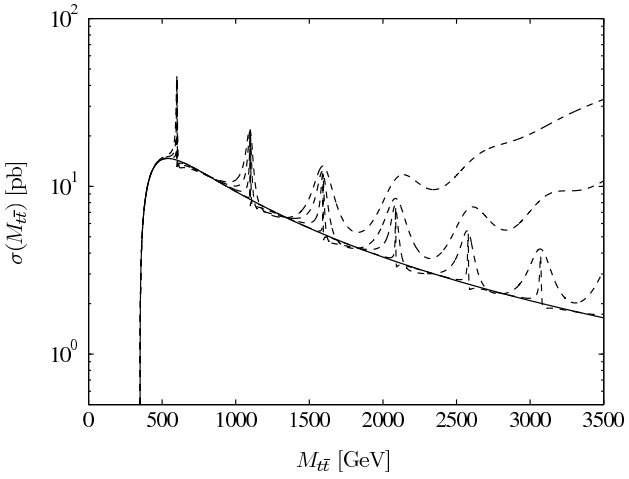

Figure 2: The dependence of the cross section of the top-antitop quark pair production by gluon fusion on the center-of-mass energy of colliding partons. The solid line and dashed lines correspond to the results of the SM and the RS model for $m_1 = 600$ GeV and $\kappa/\bar{M}_{\rm pl} = 0.01, 0.04, 0.07$ and 0.1 from bottom to top, respectively.

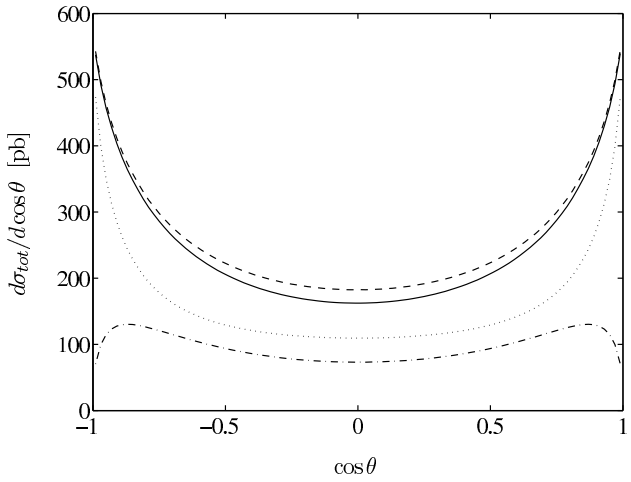

Figure 3: Differential cross section (4.1) as a function of $\cos\theta$ with $E_{CMS} = 14$ TeV for $m_1 = 600$ GeV and $\kappa/\bar{M}_{\rm pl} = 0.1$. The solid line and dashed line correspond to the results of the SM and the RS model, respectively. The differential cross sections for the like (dotted) and the unlike (dash-dotted) top-antitop spin pair productions in the RS model are also depicted.

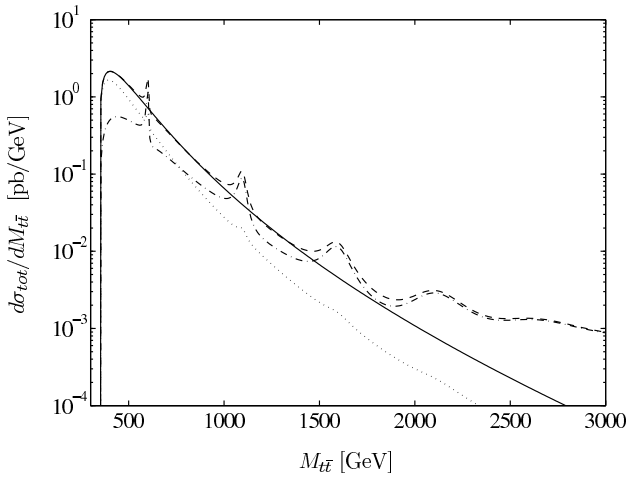

Figure 4: Differential cross section (4.2) as a function of the top-antitop invariant mass $M_{t\bar{t}}$ for $m_1 = 600$ GeV and $\kappa/\bar{M}_{\rm pl} = 0.1$. The solid and dashed lines correspond to the results of the SM and the RS model, respectively. The differential cross sections for the like (dotted) and the unlike (dash-dotted) top-antitop spin pair productions in the RS model are also depicted.

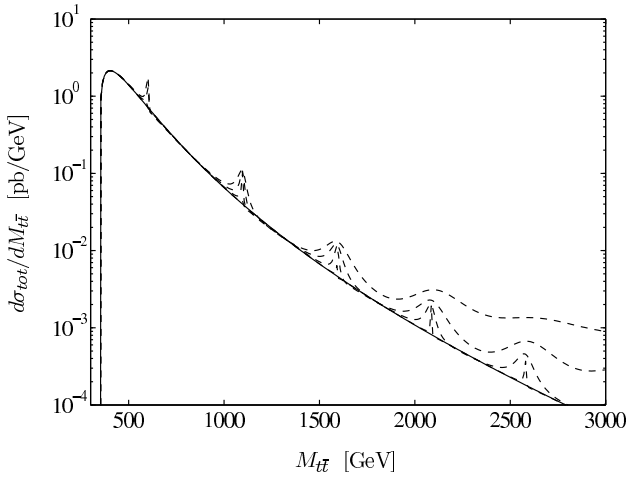

Figure 5: Differential cross section (4.2) as a function of the top-antitop invariant mass $M_{t\bar{t}}$. The solid and dashed lines correspond to the results of the SM and the RS model with $\kappa/\bar{M}_{\rm pl} = 0.01, 0.04, 0.07$ and 0.1 from bottom to top, respectively.

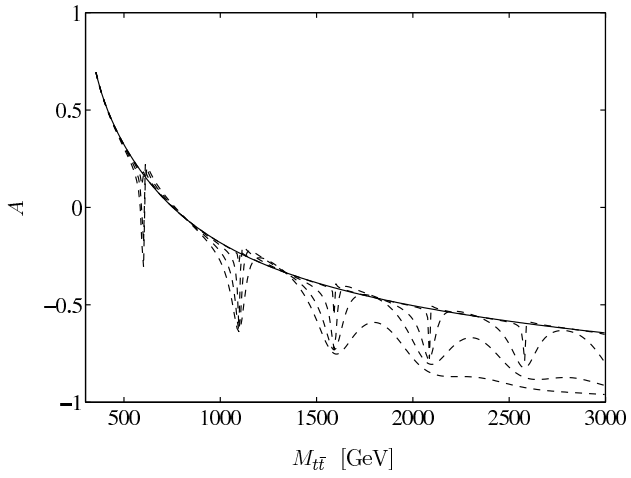

Figure 6: Spin asymmetry $\mathcal{A}$ as a function of the top-antitop invariant mass $M_{t\bar{t}}$. The solid line corresponds to the SM, while the dashed lines correspond to the RS model with $\kappa/\bar{M}_{\rm pl} = 0.01, 0.04, 0.07$ and 0.1 from up to down, respectively.

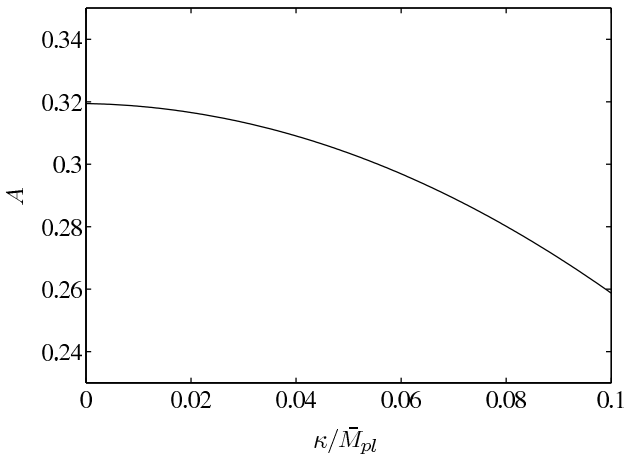

Figure 7: Spin asymmetry $\mathcal{A}$ as a function of $\kappa/\bar{M}_{\rm pl}$ at the LHC with $E_{CMS} = 14$ TeV. As $\kappa/\bar{M}_{\rm pl} \to 0$, $\mathcal{A}$ becomes the SM value, 0.319.